Maesano F.E., Toscani G., Burrato P., Mirabella F., D'Ambrogi C., Basili R. (2012). Deriving thrust fault slip rates from geological modeling: examples from the Marche coastal and offshore contraction belt, Northern Apennines, Italy. Marine and Petroleum Geology (*accepted manuscript*).

Deriving thrust fault slip rates from geological modeling: examples from the Marche coastal and offshore contraction belt, Northern Apennines, Italy

Francesco Emanuele Maesano, Giovanni Toscani, Pierfrancesco Burrato, Francesco Mirabella, Chiara D'Ambrogi and Roberto Basili

Corresponding Author: Francesco Emanuele Maesano

Email: framae80@gmail.com

Tel.: 00393805164993

Abstract

We present a reconstruction of the central Marche thrust system in the central-northern Adriatic domain aimed at constraining the geometry of the active faults deemed to be potential sources of moderate to large earthquakes in this region and at evaluating their long-term slip rates. This system of contractional structures is associated with fault-propagation folds outcropping along the coast or buried in the offshore that have been active at least since about 3Myr. The ongoing deformation of the coastal and offshore Marche thrust system is associated with moderate historical and instrumental seismicity and recorded in sedimentary and geomorphic features. In this study, we use subsurface data coming from both published and original sources. These comprise cross-sections, seismic lines, subsurface maps and borehole data to constrain geometrically coherent local 3D geological models, with particular focus on the Pliocene and Pleistocene units. Two sections crossing five main faults and correlative anticlines are extracted to calculate slip rates on the driving thrust faults. Our slip rate calculation procedure includes a) the assessment of the onset time which is based on the sedimentary and structural architecture, b) the decompaction of clastic units where

necessary, and c) the restoration of the slip on the fault planes. The assessment of the differential compaction history of clastic rocks eliminates the effects of compaction-induced subsidence which determine unwanted overestimation of slip rates. To restore the displacement along the analyzed structures, we use two different methods on the basis of the deformation style: the fault parallel flow algorithm for faulted horizons and the trishear algorithm for fault-propagation folds. The time of fault onset ranges between 5.3-2.2 Myr; overall the average slip rates of the various thrusts are in the range of 0.26-1.35 mm/yr.

Key Words: slip rate, 3D geological model, structural restoration, seismogenic source, thrust tectonics, northern Apennines, Adriatic Sea

1. Introduction

The slip rate, together with other geometrical parameters of seismogenic sources, is one ingredient of the seismic hazard models, useful for determining the activity rates of the faults, i.e. how often they generate earthquakes, and for understanding the long-term fault behavior. Slip rate calculation can be performed using different methodological approaches at different space and time scales (paleoseismological trenches, restoration of seismic exploration data, numerical modeling, GPS velocities).

The measurement of slip rates along buried or offshore tectonic structures can be carried out through the use of seismic data and exploration wells. The large amount of data for oil exploration in the Adriatic Sea and the surrounding areas, made available in part from the ViDEPI database (http://unmig.sviluppoeconomico.gov.it/videpi/en/) and in part from scientific papers, allow reconstructing three-dimensional models relative to some key chronostratigraphic horizons. In this study we investigate the area around the Conero promontory (Marche Adriatic coast, Northern Apennines, Italy), where Plio-Pleistocene

contractional tectonic structures are well known and have maximum principal stress axes oriented perpendicular to the mean structural trends (Boncio and Bracone, 2009; Heidbach et al., 2010). The ongoing activity of the more external Apennine thrust fronts is questioned on the basis of seismic line interpretations (Coward et al., 1999; Di Bucci and Mazzoli, 2002) and geomorphic analysis (Troiani and Della Seta, 2011), but is supported by historical and instrumental seismicity (Calderoni et al., 2009; Chiarabba et al., 2005) and geological-geomorphological studies (Carminati et al., 2003; Lavecchia et al., 2003, 2007; Negredo et al., 1999; Scrocca, 2006; Scrocca et al., 2007; Vannoli et al., 2004; Wegmann and Pazzaglia, 2009). Considering also the occurrence in the area of several historical and instrumental earthquakes (e.g. 1269, 1474, 1690, 1870, 1924, 1930) with $M > 5$ (see Rovida et al., 2011) and an important seismic sequence in 1972 (Console et al., 1973) many of the outer structures in the Umbria-Marche Apennines were included in the Italian database of seismogenic sources (Basili et al., 2008; DISS Working Group, 2010; see also Kastelic et al. in this issue). The capability of these thrust faults to also generate tsunamis and their potential threat level on the Adriatic coast has been evaluated by Tiberti et al. (2008).

In this study we develop a workflow for the calculation of slip rates using 3D modeling of subsurface data for the restoration of some structures that runs from the Marche coastal anticlines to the more external Apennines thrust front in the Adriatic offshore. The surrounding areas were investigated in works dealing with the identification of potential seismogenic sources (Basili and Barba, 2007; Vannoli et al. 2004) and the evolution of the external Apennines thrust fronts (Cuffaro et al. 2010; Scrocca et al. 2007). Our study focuses on the evaluation of the onset age of activity, displacement, and shortening of the thrusts. The aim of this paper is to give a quantitative estimate of slip rates for the considered time interval on thrust faults in this sector of the Umbria-Marche Apennines, some of which are

deemed to be seismogenic structures, contributing to earthquake recurrence time studies and seismic and tsunami hazard modeling.

2. Geologic and tectonic framework

The investigated area is located in the central Marche (central Italy) coastal and offshore zones (Fig. 1) and covers part of the external domain of the Umbria-Marche fold and thrust belt (Umbria-Marche Apennines). The Umbria-Marche Apennines is part of the larger Outer Northern Apennines, an arc-shaped northeast-verging thrust belt that originated in the Middle Miocene by the complex tectonic interaction between the African and European plates; this tectonic process is still active and determines active thrusting along the Adriatic coast (e.g. Barchi et al., 1998; Barchi et al., 2001; Pialli et al., 1998, Vai and Martini, 2001). The inner contractional tectonic structures have been deactivated and dissected by extensional structures which started to affect the Umbria-Marche Apennines in the Gelasian. The compression-extension pair progressively migrated in time and space from West to East generating an overprint of contractional and extensional features in adjacent regions (e.g. Barchi, 2010; Elter et al., 1975; Frepoli and Amato, 1997).

The deep and shallow geometry of the Umbria-Marche fold and thrust belt was provided by Barchi et al. (1998) and Pialli et al. (1998) using the regional seismic line CROP03 as well as by Bally et al. (1986), Coward et al. (1999) and Scarselli et al. (2007) using shorter profiles, giving different structural interpretations. Concerning the deformation style of the region, different models have been proposed: a thin-skinned model in which the contractional structures are all detached on an undeformed basement deepening from about 5 km in the Adriatic Sea to about 8 km below the Adriatic coastline and to 13-14 km below the Umbria-Marche Apennines (Bally et al., 1986); a combined thin/thick-skinned model in which the basement is partially involved in the contractional deformation and multiple

detachment levels at different depths control the development of different wavelength structures (Barchi et al., 1998) and leads to shortening rates in the order of 1.5-3.0 mm/yr (Basili and Barba, 2007); a thick-skinned model characterized by the involvement of the basement in the major thrusts which would have reactivated pre-existing Triassic faults within the basement (Coward et al., 1999; Lavecchia et al., 2003).

Reconciling these different interpretations is beyond the scopes of this work and we thus adopt the thin/thick-skinned model for which we have the largest amount of coherent data. Our study area is characterized by at least two main detachment levels that control the geometry of the contractional structures: a deep detachment located at the base of the Mesozoic-Paleogene sedimentary cover (within the Anidriti di Burano fm., Triassic evaporites) and a shallower detachment level located at the base of the Schlier fm. (Early Miocene) in the Neogene foredeep clastic successions (Barchi et al., 1998). The deep detachment controls the development of northeast-verging anticlines bounded by major thrust ramps and backthrusts, separated by wide synclines (Umbria-Marche folds). The anticlines have a wavelength of 5-10 km, and detach at a depth of 6–10 km. The shallow detachment controls the formation of short-wavelength folds (of the order of tens to hundreds of meters) detached at 2 km of depth, and involving the terrigenous foredeep and/or wedge-top successions (Barchi et al. 2001; Massoli et al. 2006). The shallow detachment level produces folds with less developed lateral continuity (non-cylindrical), a characteristic that strongly affects the thickness distribution of the Pliocene sediments deposited in the sub-basins developed in the foredeep (Argnani and Gamberi, 1995; Coward et al., 1999). Below the Umbria-Marche folds, the interpretation of the deep CROP03 seismic profile revealed that the upper part of the basement is also partly involved in the contractional structures with a wavelength of 25-35 km (Barchi et al., 1998). In the inner part of the Apennines, the Umbria-Marche folds layer comprises seven long-wavelength folds; our study area (Fig. 1) includes

the more external ones, i.e. the Coastal Anticline and the Offshore Anticline. The onset age of these two structures was constrained by the analysis of the syntectonic deposits, and is of Piacenzian (3.1 ± 0.5 Ma) and of Gelasian (2.2 ± 0.4 Ma), respectively (see Basili and Barba, 2007 for a summary).

The main terrigenous units in our study area are characterized by Neogene-Quaternary clastic wedges representing the foredeep turbidites of the Umbria-Marche Apennines. The foredeep deposits overlay a Jurassic-Paleogene multilayer known as Umbria-Marche stratigraphic succession (Cresta et al., 1989) which crops out in correspondence of the main north-east and east-verging anticlines and synclines of the Umbria-Marche Apennines to the west (Fig. 1). The lower part of the Umbria-Marche stratigraphic succession is characterized by evaporitic upper Triassic rocks, Anidriti di Burano fm. (Martinis and Pieri, 1964), overlying the basement, formed by Paleozoic and Triassic clastic rocks (continental and shallow marine environment) and metasedimentary rocks (Mirabella et al., 2008). Both the basement and evaporites do not have surface exposure in the study area and were identified in boreholes only (Anelli et al., 1994; Bally et al., 1986; Barchi et al., 1998).

The late Messinian-Quaternary sedimentary record is exposed along the Adriatic coastal belt where it is largely incomplete because of uplift and erosion. It is instead preserved in the subsurface of the Adriatic Sea and the Po Plain (Bigi et al., 1999; Calamita et al., 1999). The main events recorded by the sedimentary successions are: a sahelian cycle in the early Messinian (Ricci Lucchi, 1986a, b); a middle Messinian increment of anoxic episodes due to a crisis of salinity in the Mediterranean region with consequent evaporitic (Gessoso Solfifera fm.) sedimentation (Gelati et al., 1987); a post-evaporitic sandstones and mudstones formation up to 900 m thick (Barchi et al., 2001; Bassetti et al., 1994).

Both the Gessoso Solfifera fm. and the Messinian sediments are marked by strong angular unconformities due to sub-aerial erosion. The Pliocene succession overlies the

Messinian sediments with a low-angle unconformity which is appreciable only in seismic reflection profiles (e.g. Coward et al., 1999). In many places the Zanclean succession was completely eroded before the onset of the Piacenzian-Gelasian deposits (Calamita et al., 1999; Cantalamessa et al., 1986) which are composed of thin-bedded turbidites and can be up to 1000 m thick. The Gelasian - uppermost Pleistocene is mostly composed by epibathyal mudstones and is preserved only in wide tectonic lows between the Metauro and Esino rivers (Bally et al. 1986; Calamita et al. 1994; De Donatis and Mazzoli, 1994). In the outer Marche, the middle-upper Pleistocene fluvial and marine terraces are carved and deposited into the Piacenzian units along the Metauro River and into the Gelasian to lowermost Pleistocene units between the Metauro and Esino rivers (Elmi et al., 1987; Vannoli et al., 2004).

3. Data and Method

For this study we build up a 3D geological model using seismic and well data that come from public datasets (ViDEPI, Fantoni and Franciosi, 2010) and an original re-interpretation of published data (Esino section, Fig. 2). The data were collected with different aims and in a wide temporal range; for this reason we firstly homogenized all these datasets in terms of stratigraphy, local name of key horizons and geological age. Then we use the dataset to build a general 3D model of the area which helps us to understand the full tridimensional geometries of the observed structures. From this model we select the key structures and the best oriented sections onto which applying the restoration algorithms. As a first step of the restoration process, it is necessary to decompact the clastic sedimentary units associated with the target time interval. After decompaction, we adopt the more appropriate restoration algorithm for fault (Trishear, Fault Parallel Flow; Egan et al., 1997; Erslev, 1991; Hardy and Ford, 1997; Kane et al., 1997) and fold based on the deformation type. For each structure we determine the onset age at the site where we perform the restoration. The onset

age is defined as the maximum and minimum ages of the first stratigraphic interval affected by synsedimentary tectonics, i.e. those showing evidence of having being tilted or faulted or characterized by growth strata. The restoration then allows calculating the total amount of slip on the fault for the structure to regain the initial condition, i.e. when the reference horizon is undeformed. From this information we calculate the average slip rates from the determined onset age to present. The following sections illustrate details of the procedure and the data we used.

3.1 Geological and seismic dataset

We consider an irregular grid of seismic reflection lines crossing the study area (Fig. 1) and analyze those with the better coverage of the seismogenic sources (offshore and onshore) and the most external front of the Apennines thrust system. We also make use of isobaths and isopachs maps, publicly available in the ViDEPI database, covering the study area partly integrated with unpublished confidential data used for validation. Both isobaths and isopachs were in units of time (millisecond), so that no conversion was needed to make them consistent with the seismic reflection lines. Logs from onshore and offshore wells were used to constrain the stratigraphic properties of the sedimentary formations (Fig. 1).

The stratigraphic horizons are constructed by interpolating isobaths and seismic reflector traces (Fig. 2). Then the general structural and stratigraphic framework is interpreted using the 3D model (Fig. 3) both in map and section views.

The horizons chosen for the slip rate calculations are, whenever possible, the most recent and most continuous; namely the top of the Gessoso Solfifera fm. (Messinian; ges in Fig. 4), top Cellino unit (upper Zanclean; Dattilo et al., 1999; P1 in Fig. 4), and top of Morro d'Oro and Tortoreto units (Piacenzian; Dattilo et al., 1999; P2 in Fig. 4). Other horizons are visible within the strata of the Canzano unit (Gelasian p.p.-Pleistocene; Dattilo et al., 1999)

but they cannot be used as markers because of the lack of age constraints. For what concerns the Plio-Pleistocene interval, we take into account the chronostratigraphic subdivision of Gradstein et al. (2004) to easily compare and integrate older data; for all other purposes, we adopt the substage names and ages according to the new subdivision by Gibbard et al. (2009).

The interpretation of the seismic lines is calibrated by using the stratigraphic logs of deep wells drilled in the area. From the same logs we derive the velocity model (first column of Table 1) to convert the section from time to metric units. The seismic stratigraphy clearly shows four main lithological units (Table 1). From the bottom up they are: a) late Triassic Evaporites (Anidriti di Burano fm.; Martinis and Pieri, 1964); b) a carbonatic multilayer (Lower Jurassic - Early Oligocene); c) a middle Oligocene - upper Miocene turbiditic succession; d) the Pliocene foredeep succession. The most continuous reflectors in this stratigraphy are the Aptian - Albian Marne a Fucoidi fm. (a marly interval within the carbonatic multilayer, t fuc in Fig. 2 and Fig. 4) and the Messinian Gessoso Solfifera fm. (ges, Fig. 2). Depth conversion of relevant cross sections are obtained using the velocity intervals recorded in the deep well logs closest to each section, thereby reducing the associated uncertainty with respect of using a single velocity distribution for the entire model. The regional section from Fantoni and Franciosi (2010), named here Conero section (Fig. 4B), is already available in metric units and is thus considered as a separate dataset for comparison with other available data.

3.2 Construction of the 3D geological model and site selection

Once the homogenized tridimensional dataset is obtained (Fig. 3), we extract local 3D models (Fig. 5) of the areas selected for the decompaction procedure; then, from the decompacted models, we take 2D sections for the restoration of the remaining deformation and for slip rate calculation. To this end, we choose the following seven sites, from west to

east, (see Fig. 1 for location): Pesaro-Senigallia (PS), Conero Onshore North (ConN), Conero Onshore South (ConS), Conero Offshore North (ConM N), Conero Offshore South (ConM S), Colosseo (Col), Clara (Cl1). The chosen sites are those that have good-quality local data and are located in places that satisfy the requirement of being representative of five major thrust faults. Three of these faults have also been recognized as potential seismogenic sources and are included in the Database of Individual Seismogenic Sources (Basili et al. 2008; DISS working group, 2010): Pesaro-Senigallia ITCS032, Conero onshore ITCS008, Conero offshore ITCS031; the other two faults are characteristic of the easternmost front of the Apennines; Colosseo is a backthrust and Clara is the leading frontal thrust.

3.3 Restoration

3.3.1 Decompaction

The decompaction of sediments is necessary to remove the effects of rock volume change due to porosity reduction through time. The decompaction process backstrips a layer of sediments from the model and allows the underlying rocks to vertically decompact as a result of the overburden removal. In case of inactive anticline, strata dipping away from the anticline are generated by differential compaction of sediments onlapping the anticline limbs; in active anticlines, the observable configuration is the result of buckle folding and flexural slip as well as sediment compaction. The strain component induced by active folding adds to the strain due to differential compaction, thus increasing total stretching in syntectonic sediments (Carminati et al., 2010). We discriminate the two components of deformation and subtract the compaction effects so that the remaining vertical separation in growth strata between anticlines and synclines can be attributed to tectonic processes only (faulting and folding).

The decompaction algorithm is based on an exponentially decaying porosity with increasing depth of the sediments and follows the principles described by Sclater and Christie (1980). The effects of decompaction are more evident in syntectonic layers that were subject to differential load through time and were deformed near the free surface (where strata have relatively high porosities) and were subsequently buried to significant depths. Conversely, the effects of decompaction on displacement measurement along the fault plane are not considered for the pre-tectonic sequences because the displacement loss due to compaction is negligible (Taylor et al. 2008) and the horizon thickness is constant on both sides of the fault.

In this study, we apply the decompaction workflow to the Colosseo and Clara structures (Fig. 5) where the Plio-Pleistocene interval shows evidence of synsedimentary tectonic activity (e.g. growth strata) and thus underwent differential lithostatic load. This interval is represented by siliciclastic foredeep successions that can be assumed approximately homogeneous for original porosity and elastic properties. We model them as a sediment mixture with an equal proportion of sand and shale. We do not apply the decompaction workflow to the pre-tectonic Meso-Cenozoic carbonatic succession because it has constant thickness (e.g. no growth strata).

In our sections, the effects of decompaction are more important in the depocenters (syncline axes), where the sedimentary load is greater, than in the structural highs (anticline axes) where the sedimentary load sharply decreases. Not considering decompaction leads to an overestimation of shortening and slip on the driving thrust fault.

We extract the information from our dataset and build up a local 5-km-wide swath model (2.5 km on both sides of the trace; Fig. 5) around the section, considering that the geometry of the structures in this section is almost cylindrical for a range of few kilometers and taking into account that the section crosses the central part of the intervening structures, thereby avoiding possible boundary effects.

Figure 6b shows the effects of decompaction at the top Gelasian horizon for the Colosseo and Clara anticlines and related depocenters when the lithostatic load of the overlaying Holocene and Pleistocene sediments is removed. Overall, in the section (Fig. 6a) the measured change in thickness within the Gelasian layer ranges from a minimum of 23% in correspondence of the structural highs (ramp anticline, where the load is minimum) to a maximum of 59% in the structural lows (syncline, where the load is maximum). The average value of thickness change for the entire model is 39%.

3.3.2 Fault parallel flow, Unfolding, Trishear

Based on the type of deformation observed in each structure, the algorithms that can be used to remove the tectonic deformation are different (Fig. 5). For faulted horizons it is appropriate to use the Fault Parallel Flow (FPF) algorithm (Egan et al., 1997; Kane et al., 1997) that is designed to kinematically model hangingwall blocks where deformation is accommodated by fault-parallel shear. Where the stratigraphic horizons are not offset by the faults, but only warped by fault-propagation, the use of the trishear algorithm is instead recommended (Erslev, 1991; Hardy and Ford, 1997).

We apply the algorithms on 2D sections extracted from the 3D model. FPF is used for the restoration of the deeper and older stratigraphic markers (i.e. Marne a Fucoidi fm., Aptian-Albian; Scaglia Cinerea fm., Aquitanian; and Gessoso Solfifera fm., Messinian) in the Pesaro-Senigallia, Conero Onshore North, Conero Onshore South, Conero Offshore North and Conero Offshore South sites.

After restoring the fault plane offset, the residual deformation due to parallel folding is restored by applying the unfolding algorithm that calculates the shortening while preserving the line length of the involved horizons. We apply the unfolding procedure with respect to local pin lines relative to each structure, so the final shortening value must be

considered as related to the single fold-fault system analyzed. The values of shortening obtained by unfolding the residual deformation may include a minor slip component that we are not able to restore with FPF and a component related to the buckling and folding during contraction. We calculated both the slip-driven shortening (obtained only from the measured slip on the fault) and the total shortening which also includes the buckling and folding components.

For the Colosseo and Clara sites that are dominated by fault-propagation folding we apply the trishear method. Trishear is a kinematic model in which the decrease in displacement along the fault plane is accommodated by heterogeneous shear in a triangular zone radiating from the fault tip (Allmendinger, 1998; Zehnder & Allmendinger, 2000; Erslev, 1991). Trishear explains tectonic features that cannot be explained by self-similar, parallel-kink fold models (Suppe and Medwedeff, 1990) such as the changes in layer thickness and dip of fold forelimb, the footwall synclines, the rounded and angular fold hinges, the fold geometry and strain changes in proximity of the fault (Cardozo and Aanonsen, 2009).

The FPF, the unfolding and the trishear algorithms are applied to restore portions of the sections chosen as close as possible to structural culminations for horizons of known age, thereby providing the amount of displacement for a specific time interval and obtaining the average slip rate on the thrust planes and the relative shortening value.

4. Description and analysis of the studied structures

This section illustrates the tectonic deformation observed in the five studied structures at each site (from West to East) and the workflow used for the restoration; their correspondence with seismogenic sources of the DISS (DISS Working Group, 2010; Fig. 1) is also indicated, where applicable, by the DISS identifier (see Basili et al., 2009).

1) Pesaro-Senigallia structure (site: PS). The Esino section crosses the Pesaro-Senigallia structure not far from the coastline (Fig. 4A). The PS site is a main thrust ramp that affects the Mesozoic carbonatic succession and can be related to the southern termination of the seismogenic source ITCS032. The offset was calculated on the top of the Marne a Fucoidi fm. (Aptian-Albian) because the upward propagation of this structure into younger units is not clear. The Marne a Fucoidi reflector depicts a hangingwall anticline with a subvertical forelimb. The offset is estimated using the FPF algorithm. The unfolding procedure is then used for restoring the residual folding and calculating the relative horizontal shortening.

2 and 3) The Conero Onshore and the Conero Offshore structures are two close structural highs well imaged also by the gravimetric anomalies (ISPRA, ENI, OGS, 2009) that in this area have the highest relative values and that are affected by a sharp change with respect to the surrounding region (Fig. 7). The positive Bouguer anomaly in this area can be related with the exhumation of the Mesozoic carbonatic succession that is strongly uplifted by the Conero Onshore and Conero Offshore structures. These structures have a closure toward north-northwest, where the deformation transfers to the structures of the coastal and offshore anticlines along the coastline between Pesaro and Senigallia (ITCS032 and ITCS043). The reduction of exhumation is also imaged by the decrease of both the gravimetric gradient and the Bouguer anomalies values.

Conero onshore (sites: ConN and ConS). The northeastern part of the Esino-BR5-11 section and central part of the Conero section cross the Conero Onshore structure (ITCS008) in its northern termination (ConN) and in its central portion (ConS) respectively (Fig. 1). The ConN site (Fig. 4A) is a ramp anticline controlled by the continuation toward the north of the tectonic structure exposed in the Monte Conero area (see ConS). In this site we observe a displacement of the Messinian (ges) and Pliocene (P1, P2) stratigraphic horizons due to the propagation of a NE-verging thrust ramp probably rooted in the Mesozoic carbonatic

succession. In this case we use FPF to restore the observed deformation along the main ramp thrust. The ConS site (Fig. 4B) shows a ramp anticline with a subvertical-to-overturned forelimb. In this site the structure directly controls the exhumation of the Meso-Cenozoic succession in the Monte Conero area. In the ConS site there is a clearer geomorphic expression of the ramp anticline than in the ConN site, where the Miocene and Pliocene succession is better preserved. We restore the deformation using the FPF algorithm, applied to the Lower Jurassic marker and then unfold the residual deformation to calculate the total shortening.

Conero Offshore (site: ConM N and ConM S). The sites ConM N and ConM S represent the northern and central parts of the Conero offshore structure, respectively (ITCS031). This structure is a thrust well imaged in the ViDEPI dataset (BR9) and other data, south of the Esino-BR5-11 section (ConM N), by the presence of an important anticline. In this site, we interpret the structure as being a fault bend fold related with the northward continuation of the deeper splay imaged in the Conero Offshore South site (see ConM S). The fault bend fold offsets the Gessoso Solfifera horizons. The deformation is restored by using the FPF algorithms applied to the Gessoso Solfifera and to the top of the Scaglia Cinerea (Aquitanian) horizons, offset by the main thrust ramp, and the unfolding algorithm for the remaining deformation. In this site we do not consider the offset of secondary splays. The Conero section crosses the central part of the Conero Offshore structure. The ConM S site shows five splays; each single splay is connected to a main detachment located within the Anidriti di Burano fm. (Fig. 4B). In this site we use the Marne a Fucoidi fm. (Aptian-Albian) as a marker for the restoration because this horizon has a good lateral continuity in the section. The deformations have to be measured by backstripping each single structure, connected one by one to the main detachment. After the restoration with the FPF, we observe

a residual folding that is restored using the unfolding procedure and quantify the residual horizontal shortening of the structures.

4) Colosseo structure (site: Col). The Colosseo structure is an important backthrust connected to the main frontal thrust of the more external Clara structure (Cl1 in Fig. 1). East of the ConM S site, 20 km ENE of the Conero promontory, the Conero section crosses a NNW-SSE trending anticline related to the propagation of the backthrust. The Col site (Fig. 4B) is well imaged also by the isobaths of the base of the Pliocene (Fig. 1) and by the gravimetric data (Fig. 7). A secondary west dipping thrust is connected to the backthrust, whose offset is not significant. We model the backthrust-related fault propagation anticline and decompact the top of Pliocene by unloading the Pleistocene syntectonic succession. The decompaction reduced the vertical separation between the anticline and the adjacent basins and thereby reduced the slip on the fault plane necessary to obtain the observed deformation. After the decompaction, we apply the trishear workflow to a simplified model of the anticline and use the best fit grid values to restore the tectonic structure. The thrust controlling this anticline is not associated to any seismogenic source.

5) Clara structure (site: Cl 1). The Clara structure is related to the propagation of tectonic deformation onto the most external thrust of the Umbria-Marche belt in the Adriatic offshore. The northeastern part of the Conero section (Fig. 4B) crosses this structure in correspondence of the Clara 1 well (site Cl1). After the decompaction, the structure was restored using the trishear workflow which allows restoring all the Pliocene fault propagation folding deformation and the offset observed inside the Mesozoic carbonatic succession. This thrust system is currently not associated to any seismogenic source.

5. Results and discussion

Our results are shown in detail in Table 2 and summarized in map view in Fig. 8. For each structure we report the onset age, the total amount of slip on the thrust faults driving the deformation, the shortening driven by the slip (S.D.), the total shortening along the structures, and the slip rate averaged in the time interval from faulting onset to present. We consider all the structures as pure dip slip ramp thrust and the studied section are dip-parallel oriented so that no component of slip outside the section trace is considered.

1) Pesaro-Senigallia. We do not have specific data to address the onset age of this structure. We thus rely on the available data in the literature and adopt the age of 2.6-3.6 Myr, reported by Basili and Barba (2007) as an average value from estimations for the coastal anticline given by Argnani (1998), De Donatis et al. (1998), Coward et al. (1999) and Di Bucci and Mazzoli (2002). The amount of slip on the main thrust fault in the section is 1,339 m. Given the time of activity considered here, the average slip rate is 0.37-0.52 mm/yr. The total shortening measured along the structure is 1,985 m. This site crosses the structure near its southern termination and thus we cannot consider these values as maximum rates for the structure.

2) Conero Onshore. Data for age determination in this structure are available only in the ConN site. Here the thickness of strata in the Cellino (Zanclean) and Morro d'Oro and Tortoreto (Piacenzian) units are constant on both sides of the thrust fault. The thickness is constant also on the Canzano unit strata on the anticline back limb. These observations suggest that the activity of this structure did not begin before 2.6 Myr. Other literature data for the offshore anticline given by Argnani (1998), De Donatis et al. (1998), Coward et al. (1999) and Di Bucci and Mazzoli (2002) suggest that the activity should have started no later than 2.2 Myr. The amount of slip on the main thrust fault in the ConN site is 2,972 m and in the ConS site is 2,632 m. Given the time of activity here considered, in the ConN site the average slip rate is 1.14-1.35 mm/yr whereas in the ConS site the slip rate is 1.01-1.20

mm/yr. Both sites cross the structure near the axial culmination and we can thus consider both values as good proxies of the maximum rates for this structure. However, Fantoni and Franciosi (2010) hint at Zanclean strata onlapping the back limb of the anticline at the ConS site, which would suggest an earlier onset age (3.6 Myr) implying slower rates of deformation. The total shortening along the ConN structure is 4140 m, whilst the ConS shortening cannot be computed without considering also the ConM S thrusts.

3) Conero Offshore. In this structure the thickness of strata in the Cellino (Zanclean) unit is constant. This observation suggests that the activity of this structure did not begin before 3.6 Myr. Based on the presence of an unconformity in the Piacenzian strata we propose that the activity of this structure should have begun no later than 3.0 Myr ago. The amount of slip on the main thrust fault in the ConM N site is 1,751 m and in the ConM S is 2,741 m. Given the time of activity here considered, in the ConM N site the average slip rate is 0.49-0.58 mm/yr whereas in the ConM S site the slip rate is 0.76-0.91 mm/yr. The ConM S site crosses the structure near the axial culmination and we can thus consider these values as good proxies of the maximum rates for this structure. For the ConM N site we restore only the offset of the main thrust fault, neglecting the contribution of secondary splay faults, therefore the slip rate in this site is slightly underestimated. The total shortening measured in the ConM N is 1955 m. The shortening calculated for the ConS and ConM S structures is 7367 m.

4) Colosseo. This structure is characterized by growth strata within the Zanclean unit. We can thus assign an onset age younger than 5.3 Myr (base of Zanclean) and older than 3.6 Myr (top of Zanclean). The amount of slip on the main thrust fault in the section is 1956 m (trishear angle: 60°, P/S: 4). Given the time of activity here considered, the average slip rate is 0.37-0.54 mm/yr. The main axial culmination of this structure is located several kilometers

south of the site and the obtained rates could be much lower than the maximum rates for this structure. The total shortening is 1182 m.

5) Clara. The same observations for Colosseo can be transferred here. Considering that the Clara thrust is the upward prolongation of the basal detachment, we favor the hypothesis that Clara is slightly older than Colosseo. The amount of slip on the main thrust fault in the section is 1,385 m (trishear angle: 50°, P/S: 2). Given the time of activity considered here, the average slip rate is 0.26-0.38 mm/yr. This site crosses the structure on the axial culmination and we can thus consider these values as good proxies of the maximum rates for this structure. The total shortening is 1229 m.

Vannoli et al. (2004) calculated the slip rates of the Pesaro-Senigallia thrust, averaged on a long stretch of the northern Marche coastal belt (Fig.1), using geomorphic markers for the Upper Pleistocene and obtained slightly lower slip rate values (0.24-0.36 mm/yr) with respect to our long-term slip rates (0.37-0.52 mm/yr). Although the difference is not remarkable, it can be explained in one of two ways other than the mere fluctuation of uncertainty: 1) the slip rates were higher during the earlier stage of the fault development and progressively decreased, so that the long-term slip rates represent an average value between a faster initial phase and the slower recent activity; 2) the long-term slip rates, measured using the Marne a Fucoidi reflector which lies under the shallower detachment in the Miocene succession, is partitioned onto a few shallow anticlines above the detachment that is not totally captured by the geomorphic features used to constrain the short-term slip rate.

Overall, our reconstruction of onset ages of various thrusts suggests that the activity of the northern Apennines in the Conero area has migrated farther to the east at the end of the Messinian thereby forming the present-day leading front (Clara and Colosseo). The thrust activity has then relived (Piacenzian-Gelasian) in the west in a series of trailing younger

structures (Conero Offshore, Pesaro-Senigallia, and Conero Onshore) while, just south of our study area, the Mid-Adriatic Ridge was also forming (Scrocca, 2006).

The older offshore structures (Clara and Colosseo) are also those that recorded the least amount of slip whereas Conero Onshore, despite its younger age, is one with the highest amount of slip. Notice that Colosseo, and Conero Offshore North measuring sites cross the relevant structures very distant from their axial culmination thereby providing an underestimated value of the cumulative slip.

Overall, the calculated slip rates are distributed in the range 0.26 - 1.35 mm/yr (Fig. 8). In an ideal SW-NE profile across our study area, the calculated slip rates decrease with increasing distance from the coast, i.e. thrust faults located closer to the coast (Conero Onshore and Conero Offshore) are three-four times faster than those located far offshore (Colosseo and Clara). Clara appears to be the weakest structure because it is the oldest and slowest. Conero Onshore is instead the youngest and fastest.

On the other side of the Adriatic Sea, in the external Dinarides domain, Kastelic and Carafa (2012) obtained average long-term slip rates that also decrease with increasing distance from the coast and in the same order of magnitude of our results. This comparison suggests a similarity in mode and rate of thrusting in the two confronting thrust belts.

The Conero onshore and offshore structures are out-of-sequence thrusts with onset age significantly younger than the early outer propagation of the external fronts (e.g. Clara); our data do not allow to state if the inner and outer structures have acted contemporaneously or if their activity was asynchronous during their evolution. However, the present-day activity of the Conero onshore and offshore structures is also supported by the interpretation of seismic lines by Cuffaro et al. (2010).

In general, all the analyzed faults in our study are oriented orthogonally with respect to the present stress field (Heidbach et al., 2010, Montone et al., 2012) and the entire study

area is characterized by seismicity in the upper 10 km of the crust with magnitude up to 3.5 (Castello et al., 2006; ISIDe, 2012) and by stronger earthquakes as reported in the historical catalog (CPTI11, 2011) which suggest that all the studied structures can be considered active. The recent earthquakes of 20 and 29 May, 2012, in Emilia-Romagna, Ml 5.9 and 5.8, respectively, reactivated thrust faults (Burrato et al., 2012) in an analogous structural setting within the Outer Northern Apennines providing yet another confirmation of the ongoing activity and seismogenic potential of this type of structures.

Our results have to be considered as average slip rates from the onset time of the fault to the present assuming that all the studied faults are active. Our dataset does not allow making calculations of the differential slip rates for the Plio-Pleistocene time interval. Geologic information, with resolution higher than our data, about younger sedimentary units is needed to assess the details of the faults recent activity.

6. Conclusions

In this study we use the 3D modeling of geologic subsurface data to reconstruct the deformation history of a series of thrust-related anticlines in the central-northern Adriatic domain.

The main results of this study are:

1) The onset age of the offshore Adriatic thrust front is older than the more internal coastal structures, suggesting a possible shift of the tectonic activity toward the inner portion of the tectonic wedge, as also proposed in other studies (Cuffaro et al., 2010).

2) The Conero onshore and offshore structures show the highest deformation rates.

3) Slip rates calculated in five of the seven sites can be attributed to seismogenic sources of the DISS contributing to better characterize them. The other two calculated slip rate values,

could be used to characterize faults not yet mapped in the DISS or be used for comparison with analog thrust faults in the Apennines and other thrust belts.

Acknowledgments

The authors wish to thank the Editor Sabina Bigi, Priyank Jaiswal and an anonymous reviewer for their comments and suggestions. F. Maesano acknowledges the support of MIUR-FIRB Project "Airplane", code RBPR05B2ZJ.

Data and resources

CPTI11, the 2011 version of the Parametric Catalogue of Italian Earthquakes. Milano, Bologna, http://emidius.mi.ingv.it/CPTI.

DISS Working Group, 2010. Database of Individual Seismogenic Sources (DISS), Version 3.1.1: A compilation of potential sources for earthquakes larger than M 5.5 in Italy and surrounding areas. http://diss.rm.ingv.it/diss/, © INGV 2010 - Istituto Nazionale di Geofisica e Vulcanologia - All rights reserved.

ISIDe, 2012. Database parametrico e strumentale della sismicità italiana. http://iside.rm.ingv.it/iside/standard/index.jsp/.

ISPRA, ENI, OGS, 2009. Cartografia Gravimetrica Digitale d'Italia alla scala 1:250.000. www.isprambiente.gov.it/site/en-GB/Projects/Digital_Gravity_Maps_of_Italy_/

ViDEPI Visibilità dei dati afferenti all'attività di esplorazione petrolifera in Italia http://unmig.sviluppoeconomico.gov.it/videpi/en/

MOVE© is a registered trademark of Midland Valley Exploration Ltd..

Fault Fold© 4.5.4 is a non-commercial software from Cornell University, http://www.geo.cornell.edu/RWA/trishear/default.html

Bibliography

Allmendinger, R. W., 1998, Inverse and Forward numerical modeling of trishear fault-propagation folds. Tectonics 17, 640-656.

Anelli, L., Gorza, M., Pieri, M., Riva, M., 1994. Subsurface well data in the northern Apennines. Memorie della Società Geologica Italiana 48, 461-471.

Argnani, A., 1998. Structural elements of the Adriatic foreland and their relationships with the front of the Apennine fold-and-thrust belt. Memorie della Società Geologica Italiana 52, 647–654.

Argnani, A., Gamberi, F., 1995. Stili strutturali al fronte della catena appenninica nell'Adriatico centrosettentrionale. Studi Geologici Camerti Volume Speciale 1995/1, 19–27.

Bally, A.W., Burbi, L., Cooper, C., Ghelardoni, R., 1986. Balanced sections and seismic reflection profiles across the central Apennines. Memorie della Società Geologica Italiana 35, 257-310.

Barchi, M., 2010. The Neogene-Quaternary evolution of the Northern Apennines: crustal structure, style of deformation and seismicity. In: (Eds.) M.B., A. Peccerillo, M. Mattei, S. Conticelli, and C. Doglioni, Journal of the Virtual Explorer, volume 36, paper 10, doi: 10.3809/jvirtex.2009.00220.

Barchi, M.R., De Feyter, A., Magnani, M.B., Minelli, G., Pialli, G., Sotera, B.M., 1998. The structural style of the Umbria-Marche fold and thrust belt. Memorie della Società Geologica Italiana 52, 557–578.

Barchi, M., Landuzzi, A., Minelli, G., Pialli, G., 2001. Outer Northern Apennines. In: Anatomy of an Orogen: The Apennines and Adjacent Mediterranean Basins (G.B. Vai and I.P. Martini, eds), 215–254. Kluwer Academic Publishers, Dordrecht, The Netherlands.

Basili, R., Barba, S., 2007. Migration and shortening rates in the northern Apennines, Italy: implications for seismic hazard. Terra Nova 19, 462–468, doi: 10.1111/j.1365-3121.2007.00772.x.

Basili R., Valensise, G., Vannoli, P., Burrato, P., Fracassi, U., Mariano, S., Tiberti, M.M., Boschi, E., 2008. The Database of Individual Seismogenic Sources (DISS), version 3: summarizing 20 years of research on Italy's earthquake geology. Tectonophysics 453, 20-43, doi:10.1016/j.tecto.2007.04.014.

Basili, R., Kastelic V., Valensise G., DISS Working Group 2009, 2009. DISS3 Tutorial Series. Guidelines for Compiling Records of the Database of Individual Seismogenic Sources, Version 3. Rapporti Tecnici INGV 108, 20 pp.; http://portale.ingv.it/produzione-scientifica/ rapporti-tecnici-ingv/archivio/rapporti-tecnici-2009/.

Bassetti, M.A., Ricci Lucchi, F., Roveri, M., 1994. Physical stratigraphy of the Messinian post-evaporitic deposits in Central southern Marche area (Apennines, Central Italy). Memorie della Società Geologica Italiana 48, 275–288.

Bigi, S., Calamita, F., Cello, G., Centamore, E., Deiana, G., Paltrinieri, W., Pierantoni, P.P., Ridolfi, M., 1999. Tectonic and sedimentation within a Messinian foredeep in the Central Apennines (Italy). Journal of Petroleoum Geology, January, 22, 1, 15-18

Boncio, P., Bracone, V., 2009. Active stress from earthquake focal mechanisms along the Padan-Adriatic side of the Northern Apennines (Italy), with considerations on stress magnitudes and pore-fluid pressures. Tectonophysics 476, 180-194, doi:10.1016/j.tecto.2008.09.018.

Burrato, P., Vannoli, P., Fracassi, U., Basili, R., Valensise, G., 2012. Is blind faulting truly invisible? Tectonic-controlled drainage evolution in the epicentral area of the May 2012, Emilia-Romagna earthquake sequence (northern Italy). Annals of Geophysics, 55, 4, doi: 10.4401/ag-6182.

Calamita, F., Cello, G., Deiana, G., Paltrinieri, W., 1994. Structural styles, chronology rates of deformation and time-space relationships in the Umbria-Marche thrust system (Central Apennines, Italy). Tectonics, 13, 4, 873-881

Calamita, F., Coltorti, M., Pierantoni, P., Pizzi, A., Scisciani, V., Turco, E., 1999. Relazioni tra le faglie quaternarie e la sismicità nella dorsale appenninica umbro-marchigiana: l'area di Colfiorito. Studi Geologici Camerti, 14, 177-191.

Calderoni, G., Di Giovambattista, R., Burrato, P., Ventura, G., 2009. A seismic sequence from Northern Apennines (Italy) provides new insight on the role of fluids in the active tectonics of accretionary wedges. Earth Plan. Sci. Lett., 281, 99–109, doi:10.1016/j.epsl.2009.02.015.

Cantalamessa, G., Centamore, E., Chiocchini, U., Micarelli, A., Potetti, M., Di Lorito, L., 1986. Il Miocene delle Marche. Studi Geologici Camerti, vol. spec. “La Geologia delle Marche”, 35-55.

Cardozo, N., Aanonsen, S.I., 2009. Optimized trishear inverse modeling. Journal of Structural Geology 31, 546-560.

Carminati, E., Doglioni, C., Scrocca, D., 2003. Apennines subduction-related subsidence of Venice (Italy). Geophys. Res. Lett., 30, 1717, doi: 10.1029/2003GL017001.

Carminati, E., Scrocca, D., Doglioni, C., 2010. Compaction-induced stress variations with depth in an active anticline: Northern Apennines, Italy. J. Geophys. Res., 115, B02401, doi:10.1029/2009JB006395.

Chiarabba, C., Jovane, L., Di Stefano, R., 2005. A new view of Italian seismicity using 20 years of instrumental recordings. Tectonophysics 395, 251-268.

Console, R., Peronaci, F., Sonaglia, A., 1973. Relazione sui fenomeni sismici dell'Anconitano (1972). Annali di Geofisica, 26(4), Suppl. 1973, 3-148, DOI: 10.4401/ag-5033.

Coward, M.P., De Donatis, M., Mazzoli, S., Paltrinieri, W., Wezel, F.C., 1999. Frontal part of the northern Apennines fold and thrust belt in the Romagna-Marche arc (Italy): shallow and deep structural styles. Tectonics 18, 559–574.

Cresta, S., Monechi, S., Parisi, G., 1989. Stratigrafia del Mesozoico e Cenozoico nell'area Umbro - Marchigiana (Mesozoic - Cenozoic Stratigraphy in the Umbria - Marche area). Memorie descrittive della Carta Geologica d' Italia 39, 185 pp., 88 Fig., Roma.

Cuffaro, M., Riguzzi, F., Scrocca, D., Antonioli, F., Carminati, E., Livani, M., Doglioni, C., 2010. On the geodynamics of the northern Adriatic plate. Rendiconti Fisica Accademia Lincei 21, Suppl 1, S253–S279, doi:10.1007/s12210-010-0098-9.

Dattilo, P., Pasi, R., Bertozzi G., 1999. Depositional and structural dynamics of the Pliocene Peri-Adriatic Foredeep, NE Italy. Journal of Petroleum Geology, 22, 1, 19-36.

De Donatis, M., Mazzoli, S., 1994. Kinematic evolution of thrust-related structures in the umbro-romagnan parautochton (Northern Apennines, Italy). Terra Nova, 6, 6, 563-574

De Donatis, M., Invernizzi, C., Landuzzi, A., Mazzoli, S., Potetti, M., 1998. CROP 03: structure of the Montecalvo in Foglia-Adriatic Sea segment. Memorie della Società Geologica Italiana 52, 617–630.

Di Bucci, D., Mazzoli, S., 2002. Active tectonics of the Northern Apennines and Adria geodynamics: new data and a discussion. Journal of Geodynamics 34, 687–707.

DISS Working Group, 2010. Database of Individual Seismogenic Sources (DISS), Version 3.1.1: A compilation of potential sources for earthquakes larger than M 5.5 in Italy and surrounding areas. http://diss.rm.ingv.it/diss/, © INGV 2010 - Istituto Nazionale di Geofisica e Vulcanologia - All rights reserved.

Egan, S.S., Buddin, T.S., Kane, S.J., Williams, G.D., 1997. Three-dimensional modelling and visualization in structural geology: new techniques for the restoration and

balancing of volumes. In: Proceedings of the 1996 Geoscience Information Group Conference on Geological Visualization, Electronic Geology, 1, paper 7, 67-82.

Elmi, C., Nesci, O., Savelli, D., Maltarello, G., 1987. Depositi alluvionali terrazzati del margine adriatico appenninico centro-settentrionale: processi geomorfologici e neotettonica. Bollettino della Società Geologica Italiana 106, 717–721.

Elter, P., Giglia, G., Tongiorgi M., Trevisani, L., 1975. Tensional and compressional areas in the recent (Tortonian to present) evolution of the Northern Apennines. Bollettino di Geofisica Teorica e Applicata 42,3-18.

Erslev, E. A., 1991, Trishear fault-propagation folding. Geology 19, 6, 617-620.

Fantoni, R., Franciosi, R., 2010. Tectono-sedimentary setting of the Po Plain and Adriatic Foreland. Rendiconti di Fisica Accademia dei Lincei 21, Suppl. 1, S197–S209, doi:10.1007/s12210-010-0102-4.

Frepoli, A., Amato, A., 1997. Contemporaneous extension and compression in the Northern Apennines from earthquake fault-plane solutions. Geophysical Journal International 129, 368–388.

Gelati, R., Rogledi, S., Rossi, M., 1987. Significance of the Messinian unconformity-bounded sequences in the Apenninic margin of the Padan foreland basin, northern Italy (preliminary results). Memorie della Società Geologica Italiana 39, 319–323.

Gibbard P.L., Head M.J., Walker M.J.C. & the Subcommission on Quaternary Stratigraphy, 2009. Formal ratification of the Quaternary System/Period and the Pleistocene Series/Epoch with a base at 2.58 Ma. Journal of Quaternary Science 24, doi:10.1002/jqs.1338.

Gradstein, F.M., Ogg, J.G., Smith, A.G., Bleeker, W., Lourens, L.J., 2004. A new Geologic Time Scale, with special reference to Precambrian and Neogene. Episodes 27, 83–100.

Hardy, S., Ford, M., 1997. Numerical modelling of trishear fault-propagation folding and associated growth strata. Tectonics, 16, 5, 841-854.

Heidbach, O., Tingay, M., Barth, A., Teinecker, J., Kurfeß, D., Müller, B., 2010. Global crustal stress pattern based on the World Stress Map database release 2008. Tectonophysics 462, doi:10.1016/j.tecto.2009.1007.1023.

ISPRA, ENI, OGS, 2009. Cartografia Gravimetrica Digitale d'Italia alla scala 1:250.000. www.isprambiente.gov.it/site/en-GB/Projects/Digital_Gravity_Maps_of_Italy_/

Lavecchia, G., Boncio, P., Creati, N., 2003. A lithosperic-scale seismogenic thrust in central Italy. J. Geodyn. 36, 79–94, doi:10.1016/S0264-3707(03)00040-1.

Lavecchia, G., De Nardis, R., Visini, F., Ferrarini, F., Barbano, M.S., 2007. Seismogenic evidence of ongoing compression in eastern-central Italy and mainland Sicily: a comparison. Boll. Soc. Geol. Ital. (Ital. J. Geosci.), 126, 209–222.

Kane, S.J., Williams, G.D., Buddin, T.S., Egan, S.S., Hodgetts, D., 1997. Flexural-slip based restoration in 3D, a new approach. AAPG Annual Convention Official Program, p. A58.

Kastelic, V., Carafa, M.M.C., 2012. Fault slip rates for the active External Dinarides thrust-and-fold belt. Tectonics, 31, TC3019, doi:10.1029/2011TC003022.

Kastelic, V., Vannoli, P., Burrato, P., Fracassi, U., Tiberti, M.M., Valensise, G., 2012. Seismogenic sources in the Adriatic domain. Accepted manuscript JMPG.

Massoli, D., Koyi, H.A., Barchi, M.R., 2006. Structural evolution of a fold and thrust belt generated by multiple dècollements: analogue models and natural examples from the Northern Apennines (Italy). Journal of Structural Geology, 28, 185-199

Martinis, B., Pieri, M., 1964. Alcune notizie sulla formazione evaporitica del Triassico Superiore nell'Italia centrale e meridionale. Memorie della Società Geologica Italiana 4, 1, 649-678.

Mirabella, F., Barchi, M.R., Lupattelli, A., Stucchi, E., Ciaccio, M.G., 2008. Insights on the seismogenic layer thickness from the upper crust structure of the Umbria-Marche Apennines (Central Italy). Tectonics, 27, TC1010,doi:10.1029/2007TC002134.

Montone, P., Mariucci, M.T., Pierdominici, S., 2012. The Italian present-day stress map. Geophys. J. Int., 189, 2, 705-716, doi: 10.1111/j.1365-246X.2012.05391.x.

Negredo, A.M., Carminati, E., Barba, S., Sabadini, R., 1999. Dynamic modelling of stress accumulation in central Italy. Geophys. Res. Lett., 26, 1945–1948.

Pialli, G., Barchi, M., Minelli, G. (eds), 1998. Results of the CROP03 deep seismic reflection profile. Memorie della Società Geologica Italiana, 52, 657 pp..

Pondrelli, S., Salimbeni, S., Ekström, G., Morelli, A., Gasperini, P., Vannucci, G., 2006. The Italian CMT dataset from 1977 to the present. Physics of the Earth and Planetary Interior 159, 3-4, 286-303, doi:10.1016/j.pepi.2006.07.008.

Ricci Lucchi, F., 1986a. The foreland basin system of the northern Apennines and related clastic wedges: a preliminary outline. Giornale di Geologia 48, 3, 165-185.

Ricci Lucchi, F., 1986b. The Oligocene to recent foreland basin of the Northern Appennines. In: P.A, Allen, P., Homewood (Eds.), Foreland basins. IAS Spec. Publ., 8, 105-139.

Rovida, A., Camassi, R., Gasperini, P., Stucchi, M. (eds.), 2011. CPTI11, the 2011 version of the Parametric Catalogue of Italian Earthquakes. Milano, Bologna, http://emidius.mi.ingv.it/CPTI.

Scarselli, S., Simpson, G.D.H., Allen, P.A., Minelli, G., Gaudenzi, L., 2007. Association between Messinian drainage network formation and major tectonic activity in the Marche Apennines (Italy). Terra Nova 19, 74–81, doi: 10.1111/j.1365-3121.2006.00717.x.

Sclater, J. G., Christie, P. A. F., 1980. Continental stretching: an explanation of the post-Mid-Cretaceous subsidence of the Central North Sea Basin. Journal of Geophysical Research, 85, 3711-3739.

Scrocca, D., 2006. Thrust front segmentation induced by differential slab retreat in the Apennines (Italy). Terra Nova, 18, 154–161, doi: 10.1111/j.1365- 3121.2006.00675.x.

Scrocca, D., Carminati, E., Doglioni, C., Marcantoni, D., 2007. Slab retreat and active shortening along the central-northern Apennines. In: Thrust Belts and Foreland Basins: From Fold Kinematics to Hydrocarbon Systems (Lacombe, O., Lavé, J., Roure, F., Verges, J., eds), 471–487. Frontiers in Earth Sciences, Springer-Verlag, Berlin Heidelberg, Germany.

Suppe, J., Medwedeff, D., 1990, Geometry and kinematics of fault-propagation folding. Eclogae Geologicae Helvetiae 83, 3, 409-454.

Taylor S.K., Nicol, A., Walsh J., 2008. Displacement loss on growth faults do to sediment compation. Journal of Structural Geology 30, 394-405.

Tiberti, M. M., Lorito, S., Basili, R., Kastelic, V., Piatanesi, A., Valensise, G., 2008. Scenarios of earthquake-generated tsunamis in the Adriatic Sea. In Tsunami Science Four Years After the 2004 Indian Ocean Tsunami, Part I. Modeling, ed. P. Cummins, L. Kong, and K. Satake, Pure and Applied Geophysics Pageoph Topical Volumes Series 165, 2,117–2,142; doi: 10.1007/s00024-008-0417-6.

Troiani, F., Della Seta, M., 2011. Geomorphological response of fluvial and coastal terraces to Quaternary tectonics and climate as revealed by geostatistical topographic analysis. Earth Surf. Process. Landforms, 36, 1193-1208, doi: 10.1002/esp.2145.

Vai, G.B., Martini, I.P., 2001. Anatomy of an orogen: the Apennines and adjacent Mediterranean basins. Kluver Academic Publishers, Dordrecht/Boston/London, 632 pp.

Vannoli, P., Basili, R., Valensise, G., 2004. New geomorphic evidence for anticlinal growth driven by blind-thrust faulting along the northern Marche coastal belt (central Italy). Journal of Seismology 8, 297-312, doi:10.1023/B:JOSE.0000038456.00574.e3.

Wegmann, K.W., Pazzaglia, F.J., 2009. Late Quaternary fluvial terraces of the Romagna and Marche Apennines, Italy: Climatic, lithologic, and tectonic controls on terrace genesis in an active orogen. Quaternary Science Reviews 28, 137-165, doi: 10.1016/j.quascirev.2008.10.006.

Zehnder, A.T., Allmendinger, R.W., 2000. Velocity field for the trishear model. Journal of Structural Geology 22, 1009-1014.

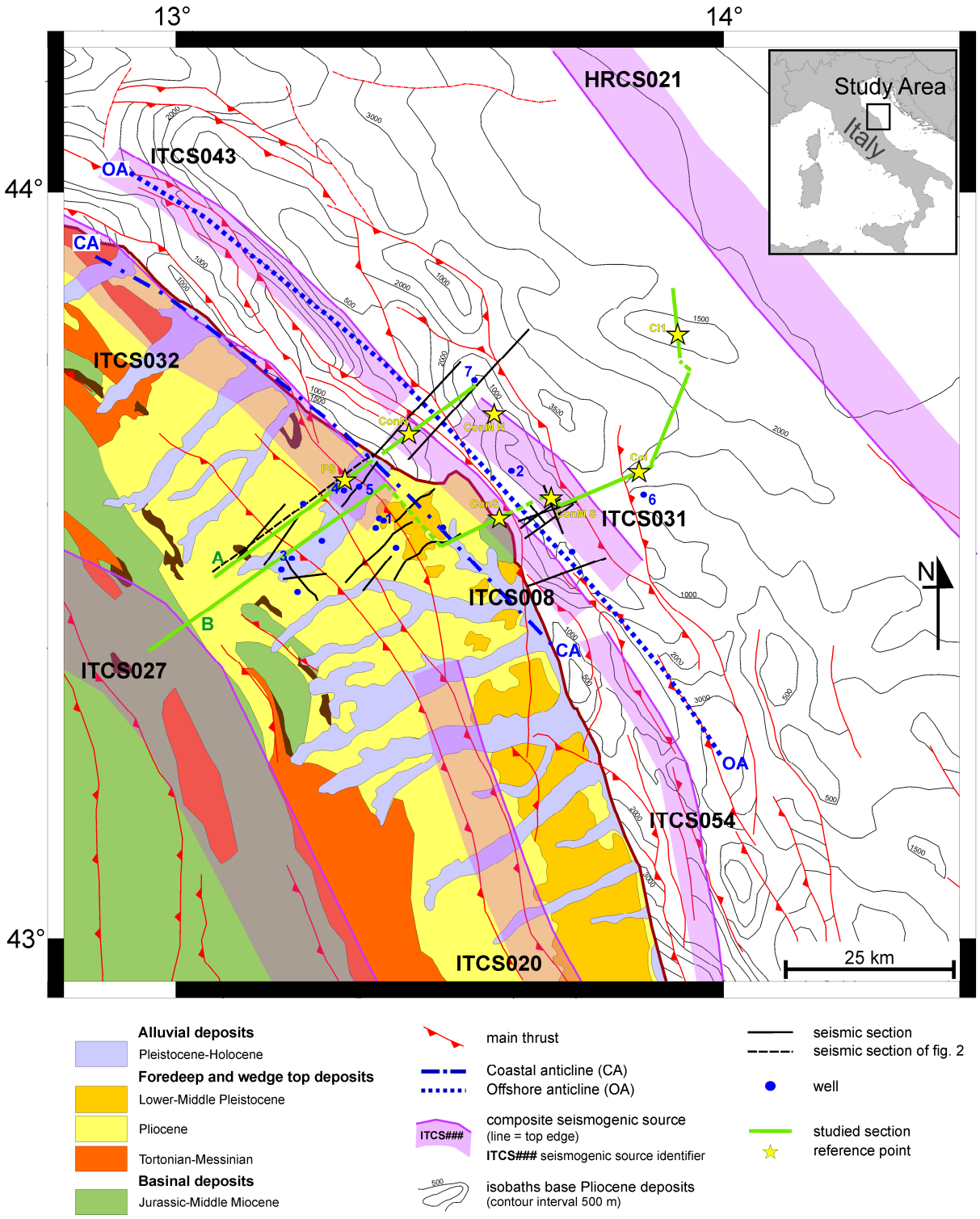

Figure 1: Map showing the main geological and structural features in and around the study area. Stars indicate the position of the reference points used to calculate the slip rates for the studied structures (PS: Pesaro-Senigallia; ConN: Conero North; ConS: Conero South; ConM N: Conero Offshore North; ConM S: Conero Offshore South; Col: Colosseo; Cl1: Clara 1). Well: 1) Offagna1, 2) Brezza1, 3) Filottrano1, 4) Chiaravalle1, 5) Monsano1, 6) Colosseo1, 7) Elga1. Cross sections: A) Esino-BR5-11 section, B) Conero section. Seismogenic source identifiers (e.g. ITCS###) as in DISS 3.1.1 (DISS Working Group, 2010).

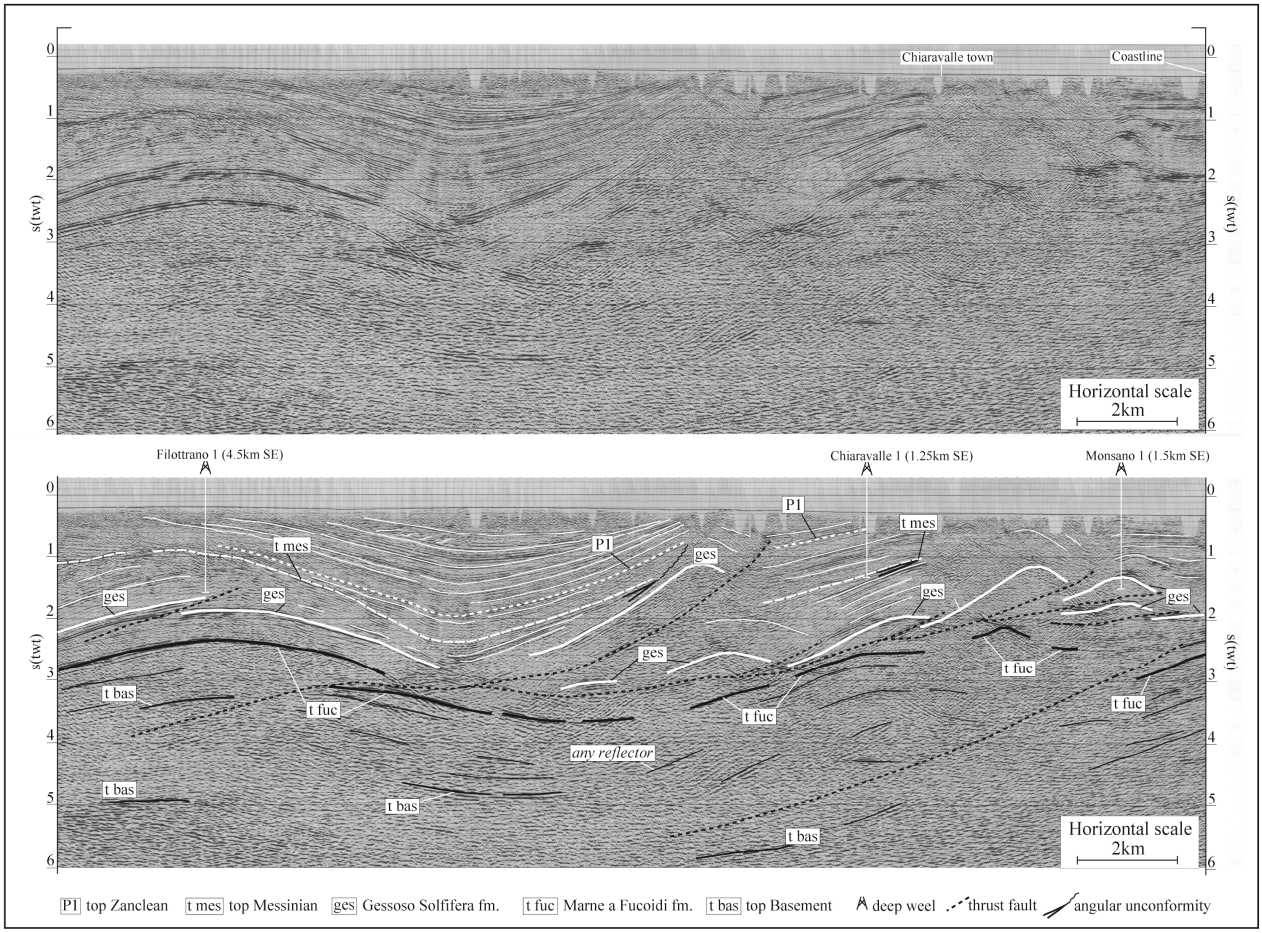

Figure 2: Seismic data (top) and geological re-interpretation (bottom) of the Esino section (after Scarselli et al., 2007) (location in figure 1) showing the geometry of the deep structures calibrated with the available boreholes and other seismic sections in the area. The section exemplifies the different styles of deformation of the deep structures with respect to the shallow structures. The deep structures involving the Umbria-Marche carbonate succession are characterized by long wavelength folds whereas the shallow structures are detached from the underlying carbonates and characterized by shorter wavelength folds.

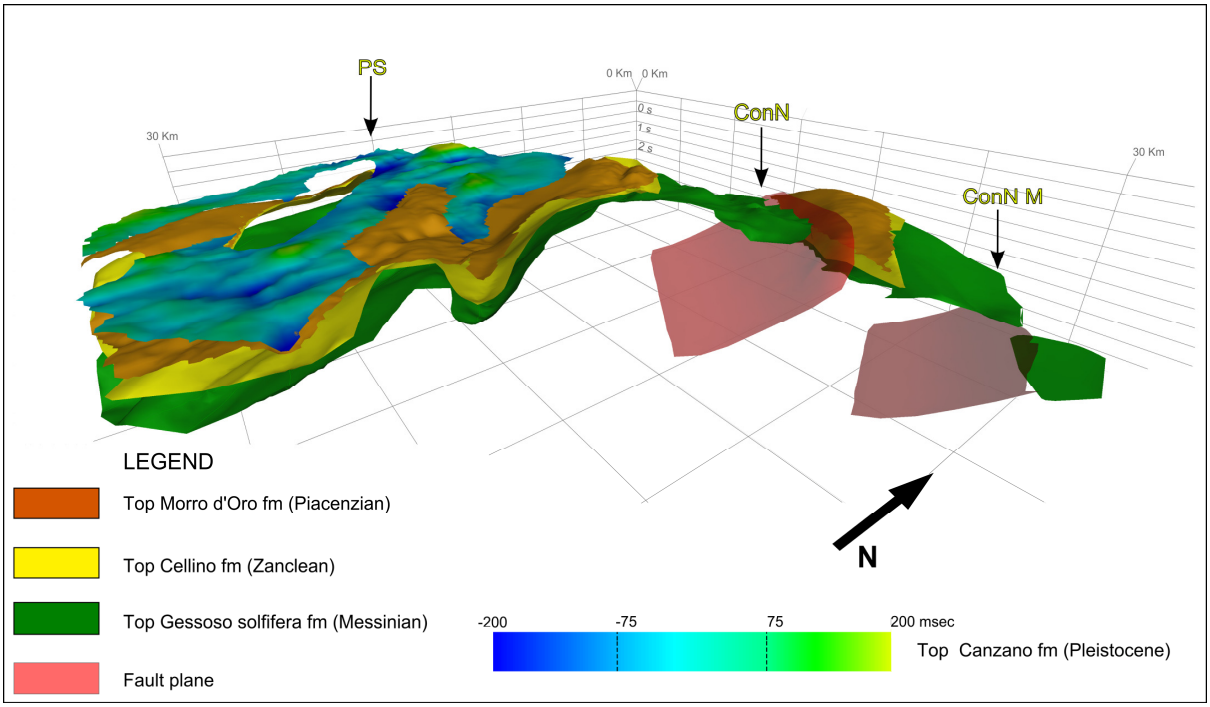

Figure 3: 3D model derived from seismic sections cross cutting the Pesaro-Senigallia (PS), Conero North (ConN) and Conero Offshore North (ConM N) structures and chrono-isobaths of Messinian-to-Pleistocene horizons.

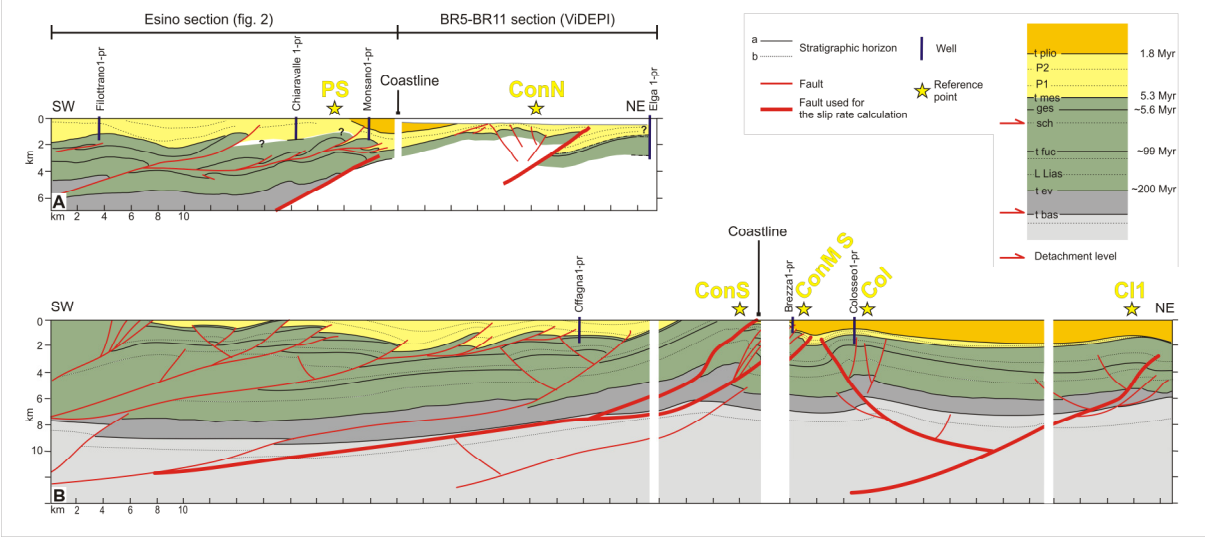

Figure 4: Geological cross sections: A) Esino-BR5-11 section, obtained from the ViDEPI database and original data (see figure 2 for seismic data and interpretation); B) Conero section, modified from line 6 in Fantoni & Franciosi (2010). Stratigraphic horizons: a) main seismic reflectors identified in all the analyzed seismic lines; b) other seismic reflectors. Simplified local stratigraphy: t bas, top of the acoustic basement; t ev, top of the Anidriti di Burano fm.; t fuc, top of the Marne a Fucoidi fm., ges, top of Messinian; P1, top of Cellino unit (Zanclean), P2, top of Morro d'Oro and Tortoreto units, (Piacenzian), t plio, Gelasian; for simplicity stratigraphic terms not cited in the text are omitted. For other symbols see figure 1.

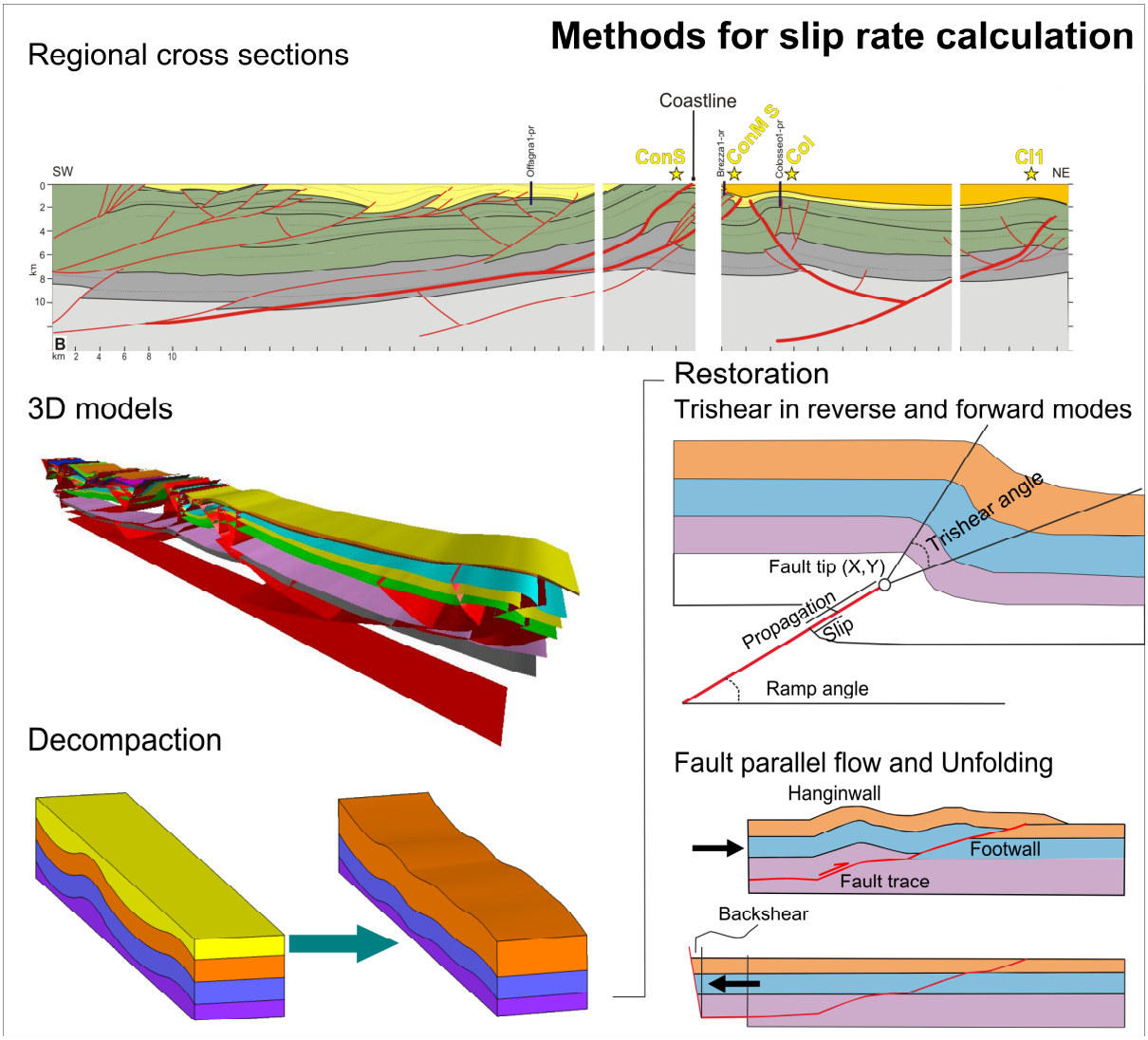

Figure 5: Workflow adopted for the slip rate calculation. Legend of the geological cross section is the same as in figure 4. The workflow uses the cross section selected from the general 3D model to build local scale tridimensional models on which the decompaction algorithm is applied (when possible). The tectonic strain is restored using trishear or fault parallel flow and unfolding algorithms. The parameters used in the trishear workflow are the fault tip coordinates (X,Y), the trishear angle, the ramp angle, the P/S ratio (propagation of the tip vs slip on the fault) and the displacement (Allmendinger, 1998; Erslev, 1991).

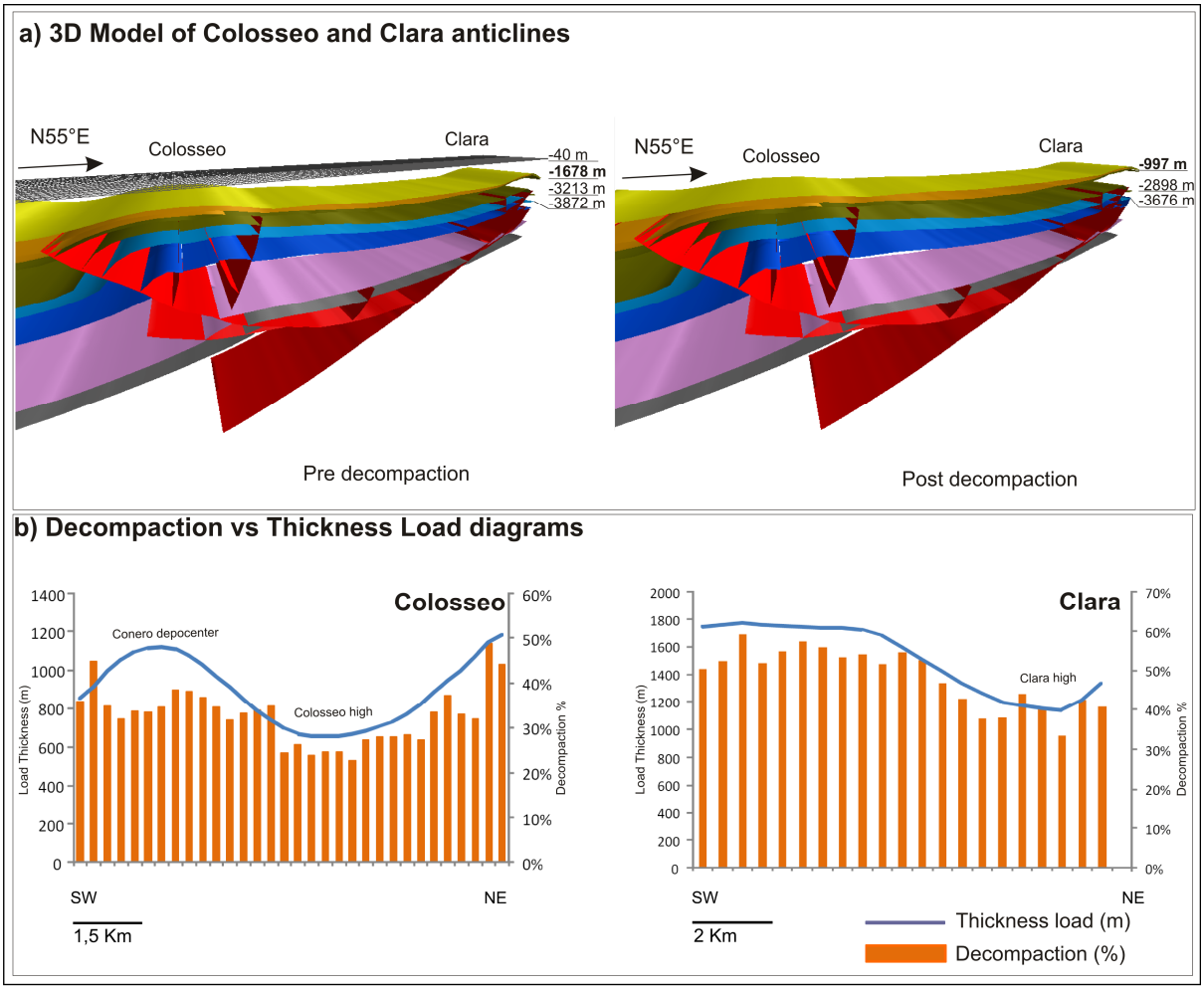

Figure 6: Decompaction data for the Colosseo and Clara 1 structures. a) Effects of the decompaction on the 3D model; the topographic relief in the Gelasian anticline is reduced after unloading the Pleistocene succession. The depth marker in the corner of the model indicate a rebound from about 1,680 m to about 1,000 m. b) the diagrams show the relationship between the thickness of the sedimentary load (e.g. the Pleistocene succession) and the amount of decompaction. Notice that in correspondence of structural highs (i.e. where load thickness is smaller) the effect of decompaction is smaller.

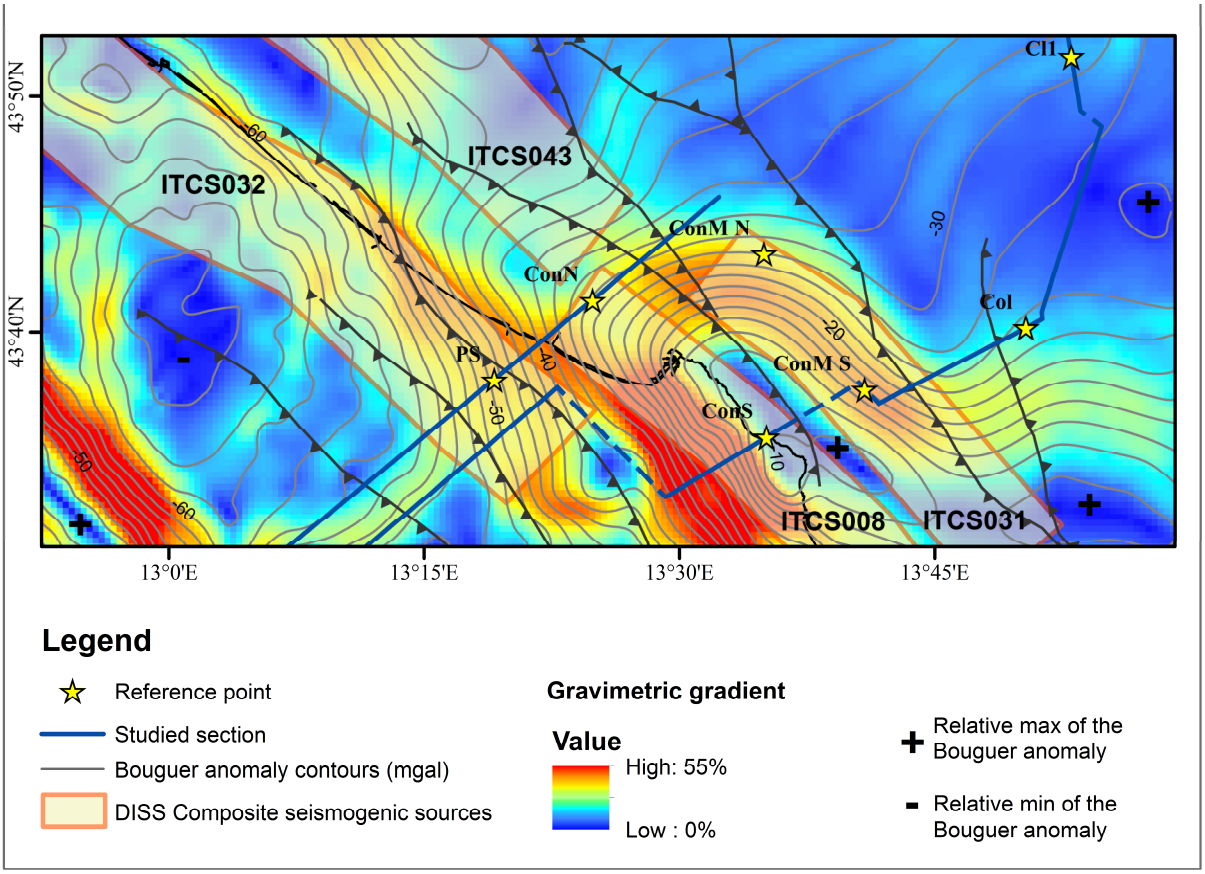

Figure 7: Gravity anomaly gradient map of the studied area obtained from spatial interpolation of the Italian Gravity Map (ISPRA, ENI, OGS, 2009). Low values (blue tones) indicate no significant variation of the gradient; high values (yellow to red tones) correspond to sharp variations of the gravimetric anomaly; the plus and minus signs indicate the relative maxima and minima of the Bouguer anomalies, respectively. Major changes in gradient roughly fit with tectonic structures. The highest anomaly and the sharper gradient are in the Conero area where the Mesozoic carbonatic succession is exhumed.

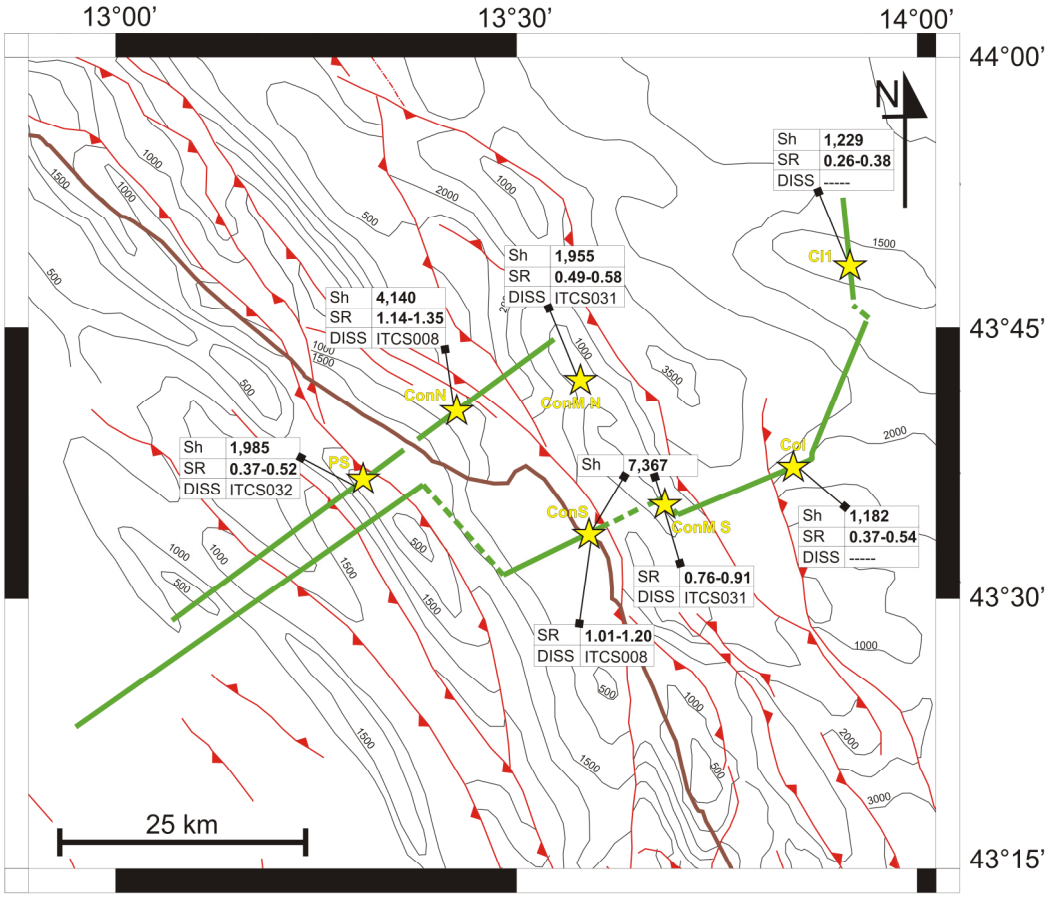

Figure 8: Synthesis map of the results of Table 2. All slip rates (SR) are in mm/yr and shortening values (Sh) are in m.

TABLES

Age / (key formations)	**L.U.**	**Interval velocity (m/s)**		
Pleistocene				
Gelasian		2,010		
Piacenzian	d		2,720	
Zanclean		2,980		
Upper-Middle Miocene / (Gessoso-solfifera)		3,395		2,980
Lower Miocene / (Schlier-Bisciaro)	c			
Oligocene				
Eocene		4,151	4,151	
Paleocene	b			
Top Lower Cretaceous / (Marne a Fucoidi fm.)				
Lias – top Lower Cretaceous		5,600	5,600	5,600
Triassic / (Anidriti di Burano)	a	6,100	6,100	6,100
Upper Paleozoic / (phyllites)		5,100	5,100	5,100
Permian / (basement rocks)		6,000	6,000	6,000

Table 1: velocity model for the Umbria-Marche succession, derived from logs of deep wells drilled in the area. Column L.U. (Litological Units) refers to the units cited in the text. The actual velocity values used for the depth conversion are those in the first column on the left of the velocity intervals.

Structure Name	Code	Coordinates (decimal degrees)		Dataset	Seismogenic source DISS	Reference horizon for restoration	Restoration method	Length (m)	Ramp dip (°)	Slip (m)	Shortening (m)		Onset age (Myr)		Slip rate (mm/yr)	
		Lat	Lon								S.D.	Total	max	min	min	max
Pesaro-Senigallia	PS	43.366	13.194	this work	ITCS032	t fuc	FPF + Unfold	13391	28	1339	1182	1985	*3.6*	*2.6*	*0.37*	*0.52*
Conero Onshore North	ConN	43.401	13.254	ViDEPI	ITCS008	ges	FPF + Unfold	19544	38	2972	2341	4140	**2.6**	*2.2*	**1.14**	*1.35*
Conero Offshore North	ConM N	43.414	13.355	ViDEPI	ITCS031	ges + Scaglia cinerea	FPF + Unfold	6658	40	1751	1341	1955	**3.6**	**3.0**	**0.49**	**0.58**
Conero Onshore South	ConS	43.336	12.353	Fantoni & Franciosi, 2010	ITCS008	Up. Lias	FPF + Unfold	20624*	30	2632	2279	7367*	**2.6**	*2.2*	**1.01**	*1.20*
Conero Offshore South	ConM S	43.354	13.412		ITCS031	t fuc			30	2741	2374		**3.6**	**3.0**	**0.76**	**0.91**
Colosseo	Col	43.376	13.511	Fantoni & Franciosi, 2010	not mapped	P1	Decomp. + Trishear	19592	53	1956	1177	1182	**5.3**	**3.6**	**0.37**	**0.54**
Clara 1	Cl1	43.492	13.544	Fantoni & Franciosi, 2010	not mapped	P1	Decomp. + Trishear	14389	38	1,385	1091	1229	**5.3**	**3.6**	**0.26**	**0.38**

Table 2: Summary of results. Reference horizons are those used for the restoration of the deformation (see figure 4). For the age of onset the maximum and minimum values are indicated (**bold** when resulting from the dataset used in this work, *italics* when adopted from literature data). Minimum and maximum slip rates result from dividing slip by the maximum and minimum age, respectively. The section length and shortening marked with * are the cumulative values for the ConS and ConM S structures.